

# Synthesis and characterization of novel Cu (II) complexes with 3-substituted-4-amino-5-mercapto-1,2,4-triazole Schiff bases: A new route to CuO nanoparticles



Hisham M. Aly, Moustafa E. Moustafa\*, Moustafa Y. Nassar, Ehab A. Abdelrahman

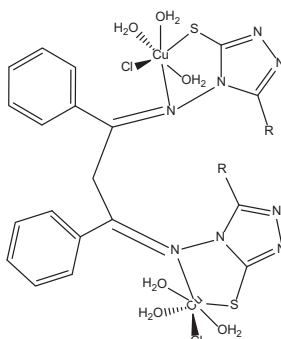
Chemistry Dept., Faculty of Science, Benha University, Benha 13518, Egypt

## HIGHLIGHTS

- New 1,2,4 triazole Schiff bases and their Cu (II) complexes have been synthesized.
- The produced Schiff bases and their complexes showed biological activities.
- CuO nanoparticles were prepared by thermal decomposition.
- The produced CuO showed catalytic activities toward MB dye.
- The as-prepared products were characterized using different analytical and spectroscopic tools.

## GRAPHICAL ABSTRACT

Proposed structure of the synthesized Cu (II) complexes.



## ARTICLE INFO

### Article history:

Received 27 December 2014  
Received in revised form 9 January 2015  
Accepted 9 January 2015  
Available online 22 January 2015

### Keywords:

1,2,4-Triazole  
Schiff base complexes  
Biological activity  
Nanoparticles  
XRD  
Photocatalytic degradation

## ABSTRACT

Cu (II) complexes, were synthesized with newly derived biologically active 1,2,4-triazole Schiff bases. The Schiff bases were synthesized by condensation of 3-substituted-4-amino-5-mercapto-1,2,4-triazole with dibenzoyl methane. The synthesized compounds were characterized using elemental analysis, magnetic moment, thermal analysis and spectral tools (FT-IR, <sup>1</sup>HNMR, ESR, and UV-Vis spectroscopy). All the synthesized complexes are nonelectrolytes in *N,N*-dimethylformamide. The synthesized Schiff bases and their Cu (II) complexes have been screened for antibacterial (*Escherichia coli* & *Staphylococcus aureus*) and antifungal (*Aspergillus flavus* & *Candida albicans*) activity using a modified Bauer-Kirby method. Interestingly, the synthesized Cu (II) complexes were used as precursors for CuO nanoparticles which were characterized using XRD, HR-TEM, FT-IR and UV-Vis spectroscopy. The photocatalytic activity of the prepared CuO nanoparticles was studied by performing the degradation of methylene blue dye under UV illumination in the presence of H<sub>2</sub>O<sub>2</sub> and the results showed that the maximum percent of the degradation of methylene blue dye (MB) was found 96.18% after 360 min.

© 2015 Elsevier B.V. All rights reserved.

## Introduction

Compounds of 1,2,4-triazole and their derivatives constitute an important class of organic compounds with diverse agricultural,

industrial and biological activities. The synthesis of such compounds has received a considerable attention in recent years [1–9]. There are numerous researches reporting the method of synthesizing 1,2,4-triazole Schiff bases and their diverse biological activities such as antioxidant, antitumor and antimicrobial. The results of these previous studies indicated that the Schiff bases

\* Corresponding author. Tel./fax: +20 13 33222578.

E-mail address: [dr.moustafa1955@yahoo.com](mailto:dr.moustafa1955@yahoo.com) (M.E. Moustafa).

possess mostly moderate to significant activities against different bacterial and fungal strains, which might be due to azomethine linkage and/or hetero atoms present in such compounds [10–15]. Moreover, transition metal complexes of triazole Schiff bases have antibacterial and antifungal activities. It is noteworthy that biological activities of the majority of the Schiff bases increased upon coordination with different transition elements. In addition, it was revealed that such compounds, which were already active, became more active and those which were not biologically active became very active upon coordination. The improvement in biological activities upon coordination may be explained on the basis of Overton's concept and chelation theory [16–28]. Copper is considered as one of the most important transition metals, which possess the ability to form biologically active coordination compounds especially with Schiff bases [29–33]. On the other hand, using coordination compounds as new precursors to produce nanosized metal oxides, were regarded as one of the most convenient and practical routes because it does not only help to avoid special instruments and complicated processes, but also it provides novel structures and good purity for the resultant products [34–46]. CuO nanoparticles play an important role among those oxides, because of its vast applications in different fields such as lithium batteries [47], Pseudo capacitors [48], and photocatalytic degradation of dyes [49–55]. Although there are several valid routes for the synthesis of CuO nanostructures such as nanocasting method, surfactant template approach, and others, those methods are complicated and/or require long time [49–59]. The numerous methods developed for the synthesis of CuO nanostructures, using the coordination compounds as precursors were considered as one of the most convenient and practical approaches [43–46]. In the present work, new bioactive triazole Schiff bases were synthesized by reacting 4-amino group of 3-substituted-4-amino-5-mercapto-1,2,4-triazole with dibenzoylmethane. These newly synthesized triazole Schiff bases were further used to react with Cu (II) to form their respective Cu (II) complexes with the hope that the produced complexes would form a novel class of metal based bioactive compounds and, moreover, may have a tendency to reduce the resistivity of bacterial/fungal strains. The synthesized triazole Schiff bases and their Cu (II) complexes were characterized by FT-IR, <sup>1</sup>HNMR, ESR, thermal analysis, molar conductance, magnetic moments, UV–Vis spectroscopy and elemental analysis data. CuO nanoparticles were synthesized through the decomposition of the corresponding Cu (II) complexes, and then their catalytic activities toward methylene blue dye (MB) have been studied under UV illumination in the presence of H<sub>2</sub>O<sub>2</sub>. The produced CuO nanoparticles were characterized by XRD, HR-TEM, FT-IR and UV–Vis spectroscopy.

## Experimental

### Materials and reagents

Copper chloride (CuCl<sub>2</sub>·2H<sub>2</sub>O) and dibenzoylmethane (PhC(OCH<sub>2</sub>COPh)) were obtained from Aldrich chemical company. All reagents were of analytical grade and they were purchased and used as received without further purification. The thiocarbohydrazide and 3-R-4-amino-5-mercapto-1,2,4-triazoles (R = H, CH<sub>3</sub> or C<sub>2</sub>H<sub>5</sub>) were prepared as reported [60–63].

### Synthesis of precursors

#### Synthesis of Schiff bases

A methanolic mixtures of 3-R-4-amino-5-mercapto-1,2,4-triazole (R = H, CH<sub>3</sub> or C<sub>2</sub>H<sub>5</sub>) and dibenzoylmethane in a 2:1 M ratio

were refluxed for 5 h in the presence of a few drops of concentrated sulfuric acid. After that, the reaction mixture was left for some time to attain the room temperature. The yellow precipitate was filtered off, washed with cold methanol and ether, recrystallized from ethanol and dried under vacuum. The prepared Schiff bases are referred to as **HL1**, **HL2** and **HL3** with 65.5%, 73.3% and 79.5% yield in case of R = H, CH<sub>3</sub> and C<sub>2</sub>H<sub>5</sub>, respectively.

*Anal. Calc.* **HL1**, C<sub>19</sub>H<sub>16</sub>N<sub>8</sub>S<sub>2</sub>, m.p. (100–104 °C), (Mwt = 420.52): C, 54.27; H, 3.84; N, 26.65; S, 15.25%. Found: C, 54.25; H, 3.85; N, 26.63; S, 15.24%. <sup>1</sup>HNMR (DMSO-d<sub>6</sub>), δ, ppm: 13.06 (s, 2H, NH), 7.30–8.20 (m, 10H, Ar–H), 4.80 (s, 2H, CH<sub>2</sub> aliphatic), 6.30 (s, 2H, H-Triazole). IR, ν, cm<sup>-1</sup>: 3400 (medium broad, NH-Triazole ring, stretching), 1625 (medium, C=N, stretching), 1260 (medium, C=S, stretching), 1575–1400 (multi bands, C=C, aromatic stretching), 785–740 (multi-bands, C–H, out of plan bending of aromatic rings).

*Anal. Calc.* **HL2**, C<sub>21</sub>H<sub>20</sub>N<sub>8</sub>S<sub>2</sub>, m.p. (190–192 °C), (Mwt = 448.57): C, 56.23; H, 4.49; N, 24.98; S, 14.30%. Found: C, 56.20; H, 4.50; N, 24.83; S, 14.27%. <sup>1</sup>HNMR (DMSO-d<sub>6</sub>), δ, ppm: 13.40 (s, 2H, NH), 7.30–8.20 (m, 10H, Ar–H), 4.80 (s, 2H, CH<sub>2</sub> aliphatic), 2.33 (s, 6H, CH<sub>3</sub>-Triazole). IR, ν, cm<sup>-1</sup>: 3460 (medium broad, NH-Triazole ring, stretching), 1620 (medium, C=N, stretching), 1265 (medium, C=S, stretching), 1575–1400 (multi bands, C=C, aromatic stretching), 785–740 (multi-bands, C–H, out of plan bending of aromatic rings).

*Anal. Calc.* **HL3**, C<sub>23</sub>H<sub>24</sub>N<sub>8</sub>S<sub>2</sub>, m.p. (110–112 °C), (Mwt = 476.63): C, 57.96; H, 5.08; N, 23.51; S, 13.46%. Found: C, 57.73; H, 4.98; N, 23.31; S, 13.29%. <sup>1</sup>HNMR (DMSO-d<sub>6</sub>), δ, ppm: 13.40 (s, 2H, NH), 7.30–8.20 (m, 10H, Ar–H), 4.80 (s, 2H, CH<sub>2</sub> aliphatic), 1.18 (t, 6H, CH<sub>3</sub>-Triazole), 2.64 (q, 4H, CH<sub>2</sub>-Triazole). IR, ν, cm<sup>-1</sup>: 3480 (medium broad, NH-Triazole ring, stretching), 1600 (medium, C=N, stretching), 1260 (medium, C=S, stretching), 1575–1400 (multi-bands, C=C, aromatic stretching), 785–740 (multi-bands, C–H, out of plan bending of aromatic rings).

### Synthesis of Cu (II) Schiff base complexes

An ethanolic solution of Schiff base (**HL1**, **HL2** or **HL3**) was refluxed with an ethanolic solution of CuCl<sub>2</sub>·2H<sub>2</sub>O in 1:1 M ratio on steam bath for 5 h. Then, to the reaction mixture 2 mmol of sodium acetate trihydrate was added and reflux was continued for 10 h. The separated complexes was filtered off, washed thoroughly with water, ethanol and ether and finally dried in vacuum over fused CaCl<sub>2</sub>.

*Anal. Calc.* Cu-**HL1**, C<sub>19</sub>H<sub>26</sub>Cl<sub>2</sub>Cu<sub>2</sub>N<sub>8</sub>O<sub>6</sub>S<sub>2</sub>, (Mwt = 724.59): C, 31.49; H, 3.62; N, 15.46; S, 8.85%. Found: C, 31.35; H, 3.77; N, 15.32; S, 8.65%. IR, ν, cm<sup>-1</sup>: 3450 (medium broad, NH-Triazole ring, stretching), 1600 (medium, C=N, stretching), 1575–1400 (multi bands, C=C, aromatic stretching), 785–740 (multi bands, C–H, out of plan bending of aromatic rings), 525 (medium, M–N, stretching).

*Anal. Calc.* Cu-**HL2**, C<sub>21</sub>H<sub>30</sub>Cl<sub>2</sub>Cu<sub>2</sub>N<sub>8</sub>O<sub>6</sub>S<sub>2</sub>, (Mwt = 752.64): C, 33.51; H, 4.02; N, 14.89; S, 8.52%. Found: C, 33.37; H, 4.11; N, 14.90; S, 8.54%. IR, ν, cm<sup>-1</sup>: 3450 (medium broad, NH-Triazole ring, stretching), 1605 (medium, C=N, stretching), 1575–1400 (multi bands, C=C, aromatic stretching), 785–740 (multi bands, C–H, out of plan bending of aromatic rings), 522 (medium, M–N, stretching).

*Anal. Calc.* Cu-**HL3**, C<sub>23</sub>H<sub>34</sub>Cl<sub>2</sub>Cu<sub>2</sub>N<sub>8</sub>O<sub>6</sub>S<sub>2</sub>, (Mwt = 780.69): C, 35.38; H, 4.39; N, 14.35; S, 8.21%. Found: C, 35.30; H, 4.41; N, 14.59; S, 8.24%. IR, ν, cm<sup>-1</sup>: 3460 (medium broad, NH-Triazole ring, stretching), 1597 (medium, C=N, stretching), 1575–1400 (multi bands, C=C, aromatic stretching), 785–740 (multi bands, C–H, out of plan bending of aromatic rings), 520 (medium, M–N, stretching).

## Synthesis of nanosized CuO

The as-prepared Cu (II) complexes were thermally decomposed for 2 h at 650 °C in an open air electric furnace to produce CuO nanoparticles.

## Physical measurements

FT-IR spectra of Schiff bases, their Cu (II) complexes and Copper oxides were recorded on a Nicolet iSio FT-IR spectrophotometer in the 4000–400  $\text{cm}^{-1}$  region in KBr disks. Electronic spectra of the complexes were recorded in *N,N*-dimethylformamide (DMF) and Nujol oil on Jasco (V-530) UV-Vis spectrophotometer. The  $^1\text{H}$ NMR spectra of Schiff bases were recorded in DMSO on a Bruker 300 MHz spectrometer at room temperature using TMS as an internal reference. Differential thermal and thermogravimetric analysis (DTA-TG) of the prepared Cu (II) complexes, measured from room temperature to 1000 °C at a heating rate of 10 °C  $\text{min}^{-1}$ , were obtained using Shimadzu TA-60 WS thermal analyzer. Elemental analyses for C, H, N, and S were done using Elementer Vario EL III Carlo Erba 1108 instrument. ESR of Cu (II) complexes was recorded on Varian E-9 spectrophotometer. Molar conductivity measurements of the complexes were recorded on an YSI conductivity bridge with a cell having cell constant 1. X-ray powder diffraction (XRD) of the as-prepared copper oxides were recorded on a 18 kW diffractometer (Bruker; model D8 Advance) with monochromated Cu  $K\alpha$  radiation ( $\lambda$ ) 1.54178 Å. The HR-TEM images were taken on a transmission electron microscope (JEOL; model 1200 EX) at an accelerator voltage of 220 kV. The molar magnetic susceptibility;  $\chi_M$  of the synthesized Cu (II) complexes was measured using Gouy balance at room temperature. The sample was packed in a Gouy tube of known mass. Mercury (II) tetrathiocyanatocobaltate [ $\text{Hg}\{\text{Co}(\text{SCN})_4\}$ ] was used for the calibration of the Gouy tube. The obtained values were corrected for diamagnetism using Pascal's constants.

## Biological activity

Antimicrobial activities of Schiff bases, their Cu (II) complexes and as-prepared CuO nanoparticles were determined using a modified Bauer-Kirby method [64]. Briefly, 100  $\mu\text{L}$  of the pathogenic bacteria/fungi were grown in 10 mL of fresh media until they reached a count of 108 cells/mL for bacteria or 105 cells/mL for fungi [65]. 100  $\mu\text{L}$  microbial suspensions were spread onto agar plates corresponding to the both pathogens in which they were maintained. Isolated colonies of each organism were selected and tested for susceptibility by disc diffusion method. A filter paper disc impregnated with the tested chemical was placed on agar. Plates with fungi (*Aspergillus flavus* and *Candida albicans*) were incubated at 25–27 °C for 24–48 h. whereas, plates with gram negative bacteria (*Escherichia coli*)/gram positive bacteria (*Staphylococcus aureus*) were incubated at 35–37 °C for 24–48 h. The diameter of the inhibition zone was measured in millimeters.

## Photocatalytic activity measurements

The photocatalytic degradation of methylene blue dye (MB) solution is performed using CuO sample prepared using Cu (II)-**HL3**. For a typical photocatalytic experiment, 100 mg of the prepared photocatalyst is added to 50 mL of 10 mg/L aqueous dye solution. The solution in which the prepared photocatalysts are dispersed is first kept in the dark for 2 h to allow the system to reach an adsorption-desorption equilibrium. Afterwards, 2 mL of 0.2 M  $\text{H}_2\text{O}_2$  solution was added and UV light (at 365 nm) irradiation of the solution is started. The degradation was investigated in a Pyrex beaker under the UV illumination using a 250 W xenon arc lamp (Thoshiba, SHLS-002) ( $\lambda = 365 \text{ nm}$ ). After recovering the catalyst by centrifugation, the light absorption of clear solution is

measured at 664 nm ( $\lambda_{\text{max}}$  for MB) at a set time using a UV-Vis spectrophotometer.

## Results and discussion

### Synthesis and characterization of **HL1**, **HL2** and **HL3** Schiff bases

New triazole Schiff bases were synthesized by the reaction of 3-*R*-4-amino-5-mercapto-1,2,4-triazole ( $R = \text{H}, \text{CH}_3$  or  $\text{C}_2\text{H}_5$ ) with dibenzoylmethane in 2:1 ratio as shown in Scheme 1. Characterization of the synthesized Schiff bases was carried out by m.p., FT-IR,  $^1\text{H}$ NMR and elemental analysis. The C%, H%, N% and S% obtained from elemental analysis are in excellent agreement with the proposed molecular formulas.

### FT-IR spectra of **HL1**, **HL2** and **HL3** Schiff bases

In the FT-IR spectra of the synthesized Schiff bases (Fig. 1), a medium intensity broad band observed in the range of 3500–3100  $\text{cm}^{-1}$  is attributed to NH stretching of the triazole ring whereas, a medium to high intensity band observed in the range of 1625–1600  $\text{cm}^{-1}$  is attributed to C=N stretching. The absorption at about 1260  $\text{cm}^{-1}$  can be assigned to C=S stretching. Various absorption bands observed in the range of 1575–1400  $\text{cm}^{-1}$  are assigned to C=C aromatic stretching vibrations whereas, bands observed in the range of 785–740  $\text{cm}^{-1}$  are assigned to C–H out of plane bending of aromatic rings [66–68].

### $^1\text{H}$ NMR spectra of **HL1**, **HL2** and **HL3** Schiff bases

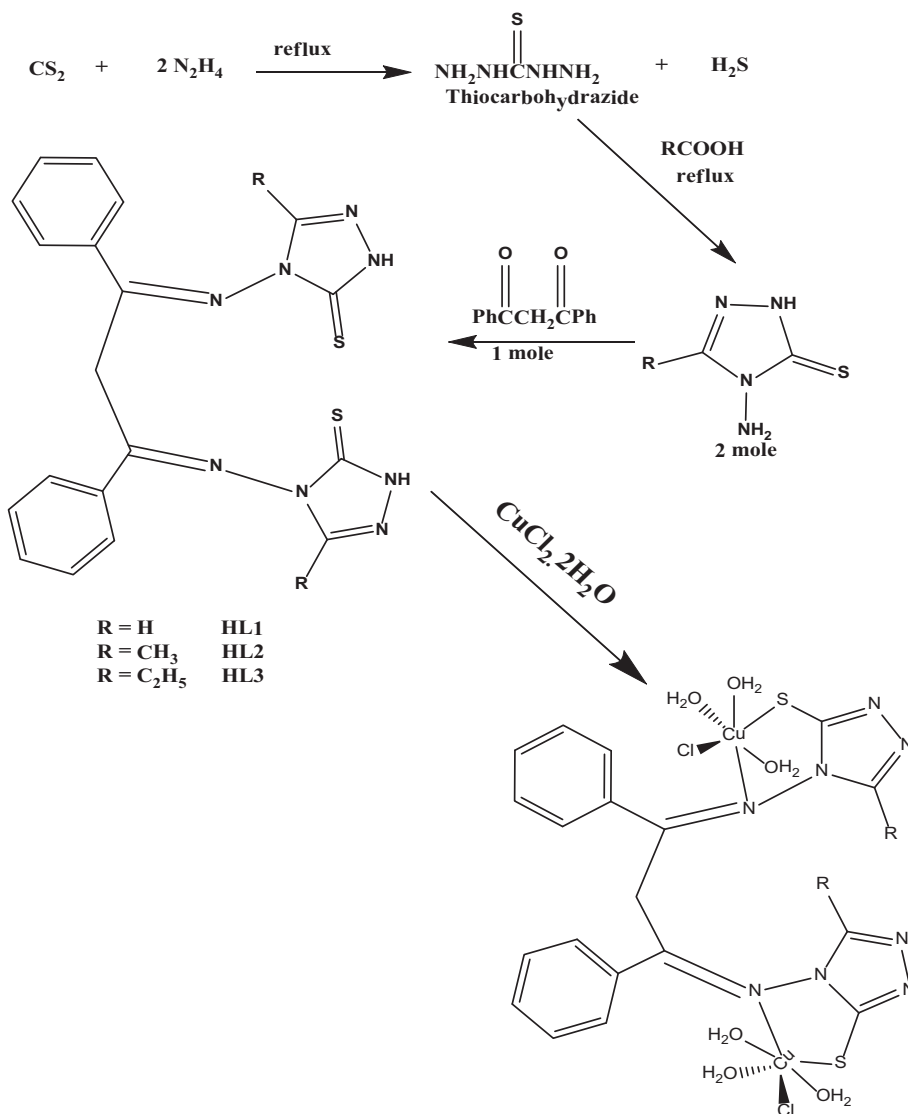
The  $^1\text{H}$ NMR spectra (in  $d_6$ -DMSO) of the synthesized Schiff bases have signals at about: 13.40 (s, 2H, NH) (**HL2** and **HL3**), 13.06 (s, 2H, NH) (**HL1**), 7.30–8.20 (m, 10H, Ar–H), 4.80 (s, 2H,  $\text{CH}_2$  aliphatic), 6.30 (s, 2H, H-Triazole-**HL1**), 2.33 (s, 6H,  $\text{CH}_3$ -Triazole-**HL2**), 1.18 (t, 6H,  $\text{CH}_3$ -Triazole-**HL3**) and 2.64 (q, 4H,  $\text{CH}_2$ -Triazole-**HL3**) [69]. The existence of NH on the triazole ring also was proved through its disappearance in  $^1\text{H}$ NMR ( $d_6$ -DMSO- $\text{D}_2\text{O}$ ).

### Synthesis and characterization of Cu (II) Schiff base complexes

Solid Cu (II) Schiff base complexes were synthesized by allowing the synthesized Schiff bases to react with  $\text{CuCl}_2 \cdot 2\text{H}_2\text{O}$  in 1:1 ratio. All the synthesized Cu (II) complexes are stable at room temperature, nonhygroscopic and soluble in DMF and DMSO. The synthesized Cu (II) complexes were characterized using elemental analysis, molar conductivity, FT-IR, magnetic moment, ESR, DTG analysis, and UV-Vis spectroscopy. The elemental analyses of Cu (II) complexes are in excellent agreement with the proposed molecular formulas. The structure of the Cu (II) complexes are shown in Scheme 1. The molar conductivity measurements at  $10^{-3}$  M in DMF indicate that these complexes are nonelectrolytes.

### FT-IR spectra of Cu (II) Schiff base complexes

In the FT-IR spectra of the synthesized Schiff bases, a medium intensity broad band observed in the range of 3500–3400  $\text{cm}^{-1}$  is attributed to NH stretching of the triazole ring. This band was observed in all the complexes (Fig. 1) in the range of 3450–3460  $\text{cm}^{-1}$ , confirming that NH is not involved in coordination. A medium to high intensity band in the range of 1625–1600  $\text{cm}^{-1}$  is attributed to C=N stretching which shifts lower by 20–25  $\text{cm}^{-1}$  to 1602–1580  $\text{cm}^{-1}$  after coordination. This supports Schiff base coordination to Cu (II) through the nitrogen atom of C=N group. This is further supported by the appearance of a medium intensity band in the range of 525–520  $\text{cm}^{-1}$  which assigned to Cu–N stretching [70]. The characteristic absorption at about 1260  $\text{cm}^{-1}$  for C=S group disappeared after coordination and this confirming that; sulfur atom is involved in coordination.



**Scheme 1.** Synthesis of 3-R-4-amino-5-mercapto-1,2,4-triazole Schiff bases (**HL1**, **HL2** and **HL3**) and their Cu (II) complexes.

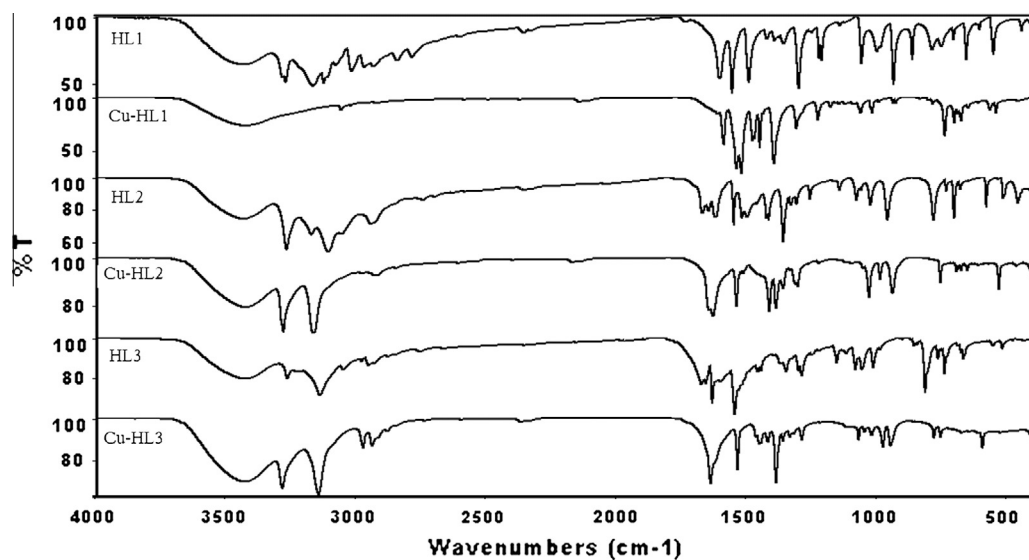


**Fig. 1.** FT-IR of Schiff bases (**HL1**, **HL2** and **HL3**) and their Cu (II) complexes.

### Electronic spectra of Cu (II) Schiff base complexes

In octahedral crystal field, the ground state electronic distribution of  $\text{Cu}^{2+}$  is  $t_{2g}^6 e_g^3$  which yields  ${}^2E_g$  term whereas, the excited electronic state is  $t_{2g}^5 e_g^4$  which corresponds to  ${}^2T_{2g}$  term. Thus only one single electron transition, i.e.,  ${}^2E_g \rightarrow {}^2T_{2g}$ , is expected in an octahedral crystal field. Octahedral coordination is distorted either by elongation or compression leading to tetragonal symmetry. Normally, the ground  ${}^2E_g$  state is split due to Jahn–Teller effect and hence lowering of symmetry is expected for Cu (II) ion. Thus,  ${}^2E_g$  state splits into  ${}^2B_{1g}(\mathbf{d}_{x^2-y^2})$  and  ${}^2A_{1g}(\mathbf{d}_{z^2})$  in tetragonal symmetry whereas, the excited term  ${}^2T_{2g}$  also splits into  ${}^2B_{2g}(\mathbf{d}_{xy})$  and  ${}^2E_g(\mathbf{d}_{xz}, \mathbf{d}_{yz})$ . Electronic spectra of Cu (II) complexes exhibit broad bands in the range of 14,598–14,947  $\text{cm}^{-1}$  with a shoulder on the low energy side at the range of 11,587–11,820  $\text{cm}^{-1}$ , which can be assigned respectively to  ${}^2B_{1g} \rightarrow {}^2E_g$  and  ${}^2B_{1g} \rightarrow {}^2A_{1g}$  transition in a tetragonally distorted octahedral configuration as shown in Table 1 [70].

### Magnetic studies and conductivity measurements of Cu (II) Schiff base complexes

The magnetic measurements for Cu (II)-**HL1**, Cu (II)-**HL2**, and Cu (II)-**HL3** complexes are 1.76, 1.82 and 1.86 B.M., respectively, which regarded slightly higher than the spin only value 1.73 B.M. expected for one unpaired electron [70] whereas the molar conductivity values, 24, 24 and 28  $\Omega^{-1} \text{cm}^2 \text{mol}^{-1}$ , respectively, indicates the non-electrolyte nature of such complexes [70].

### ESR of Cu (II) Schiff bases complexes

Electron Spin Resonance (ESR) is a branch of spectroscopy in which radiation of microwave frequency is absorbed by molecules possessing electrons with unpaired spins [71]. This method is an essential tool for the analysis of the structure of molecular systems or ions containing unpaired electrons, which have spin-degenerate ground states in the absence of magnetic field. In the study of solid state materials, ESR method is employed to understand the symmetry of surroundings of the paramagnetic ion and the nature of its bonding to the nearest neighboring ligands. When a paramagnetic substance is placed in a steady magnetic field (H), the unpaired electron in the outer shell tends to align with the field. So the two fold spin degeneracy is removed. Thus the two energy levels,  $E_{1/2}$  and  $E_{-1/2}$  are separated by  $g\beta H$ , where  $g$  is spectroscopic splitting factor and is called gyro magnetic ratio which was divided into two types ( $g_{11}$  (in z-direction) and  $g_{\perp}$  (in x or y-direction)) and  $\beta$  is the Bohr magneton. Since there is a finite probability for a transition between these two energy levels, a change in the energy state can be stimulated by an external radio frequency. When microwave frequency ( $\nu$ ) is applied perpendicular to the direction of the field, resonance absorption will occur between the two split spin levels. The resonance condition is given by,  $h\nu = g\beta H$ , where  $h$  is Planck's constant. ESR results give rise to a new parameter,  $G$  which is defined as:

$$G = \frac{g_{11} - g_e}{g_{\perp} - g_e} \quad (1)$$

**Table 1**  
Electronic absorption spectral data of the synthesized Cu (II) complexes.

Complex	CT band		d → d bands		Assignment
	Nujol mull	DMF	Nujol mull	DMF	
Cu- <b>HL1</b>	26,891	28,169	11,820	11,120	${}^2B_{1g} \rightarrow {}^2A_{1g}$
			14,947	15,421	${}^2B_{1g} \rightarrow {}^2E_g$
Cu- <b>HL2</b>	30,328	28,328	11,820	11,786	${}^2B_{1g} \rightarrow {}^2A_{1g}$
			14,598	13,985	${}^2B_{1g} \rightarrow {}^2E_g$
Cu- <b>HL3</b>	25,954	28,011	11,587	11,976	${}^2B_{1g} \rightarrow {}^2A_{1g}$
			14,619	14,867	${}^2B_{1g} \rightarrow {}^2E_g$

The ESR spectrum of the prepared Cu (II) complexes shows  $g_{11} > g_{\perp} > g_e$  (2.0023) as shown in Fig. 2 and Table 2. This indicates that tetragonal elongation distortion is predominant and hence, the unpaired electron is localized in the ( $\mathbf{d}_{x^2-y^2}$ ) orbital. The  $G$  parameter observed for these complexes is less than 4 indicating exchange interaction in the solid complexes, consistent with distorted octahedral configuration [71]. The optical absorption and ESR data in tetragonal elongation distortion are related as follows,

$$\begin{aligned} g_{11} &= g_e - \frac{8\lambda}{\Delta E_{11(xy)}({}^2B_{1g} \rightarrow {}^2B_{2g}) = \Delta_{11}} g_{\perp} \\ &= g_e - \frac{2\lambda}{\Delta E_{\perp(xy,yz)}({}^2B_{1g} \rightarrow {}^2E_g) = \Delta_{\perp}} \end{aligned} \quad (2)$$

where  $\lambda$  is the spin-orbit coupling constant for free Cu (II) ion =  $-830 \text{cm}^{-1}$ . The calculated  $\Delta E$  values are summarized in Table 2.

Further, if  $A_{11}$ ,  $g_{11}$  and  $g_{\perp}$  values are known,  $\alpha^2$  (covalency parameter) can be estimated using the equation

$$\alpha^2 = (A_{11}/0.036) + (g_{11} - 2.0023) + 3/7(g_{\perp} - 2.0023) + 0.04 \quad (3)$$

### Thermogravimetric and differential thermal analysis of Cu (II) Schiff base complexes

TG and DTG curves (Fig. 2) for Cu-**HL3** Schiff base complex showed two decomposition steps. The first exothermic step in the temperature range 24–315 °C can be attributed to the loss of six coordinated water molecules and  $\text{Cl}_2$  with a weight loss of 22.86% (calc. 23.00%) whereas, the second exothermic step in the temperature range 315–522 °C can be attributed to the loss of organic moiety with a weight loss of 60.00% (calc. 60.87%). Above 522 °C, Cu (II) complexes were decomposed to their respective oxide (CuO). The theoretical percent of copper was 16.27% (calc. 17.14%) [70].

### Synthesis and characterization of CuO nanoparticles

Solid Cu (II) complexes were ignited at 650 °C to produce the corresponding copper oxide (CuO), which were characterized using XRD, HR-TEM, FT-IR and optical properties. By this fast and simple method, CuO nanoparticles can be produced without expensive and toxic solvents or complicated equipment.

### XRD and HR-TEM of CuO

The crystalline structures of CuO samples were characterized using XRD as shown in Fig. 3. All these diffraction peaks, including not only the peak positions but also their relative intensities, can be perfectly indexed into the monoclinic phase of CuO with cell constants:  $a = 4.678 \text{Å}$ ,  $b = 3.431 \text{Å}$  and  $c = 5.136 \text{Å}$  (space group C2/c, JCPDS card 80-0076); these data are in agreement with the ones published by Chickneyan et al. [72]. No characteristic peaks of other impurity phases have been detected, indicating that the final product is of high purity. The average crystal size was estimated using the Debye–Scherrer formula [73,74]:

$$D = 0.9\lambda/\beta \cos \theta_B$$

where  $\lambda$ ,  $\beta$ ,  $\theta_B$  are the X-ray wavelength, the full width at half maximum (FWHM) of the diffraction peak and the Bragg diffraction angle, respectively. The estimated crystal size of CuO samples, prepared using Cu (II) complexes of **HL1**, **HL2** and **HL3**, using XRD data was found 35.60, 34.47 and 28.28 nm, respectively. Whereas, particle size was supported using HR-TEM (cubic, sphere and irregular shaped aggregates with average particle size of 26.75, 33.45 and 27.15 nm, respectively) as shown in Fig. 3. Diffraction patterns obtained from both of HR-TEM and XRD showed exactly the same

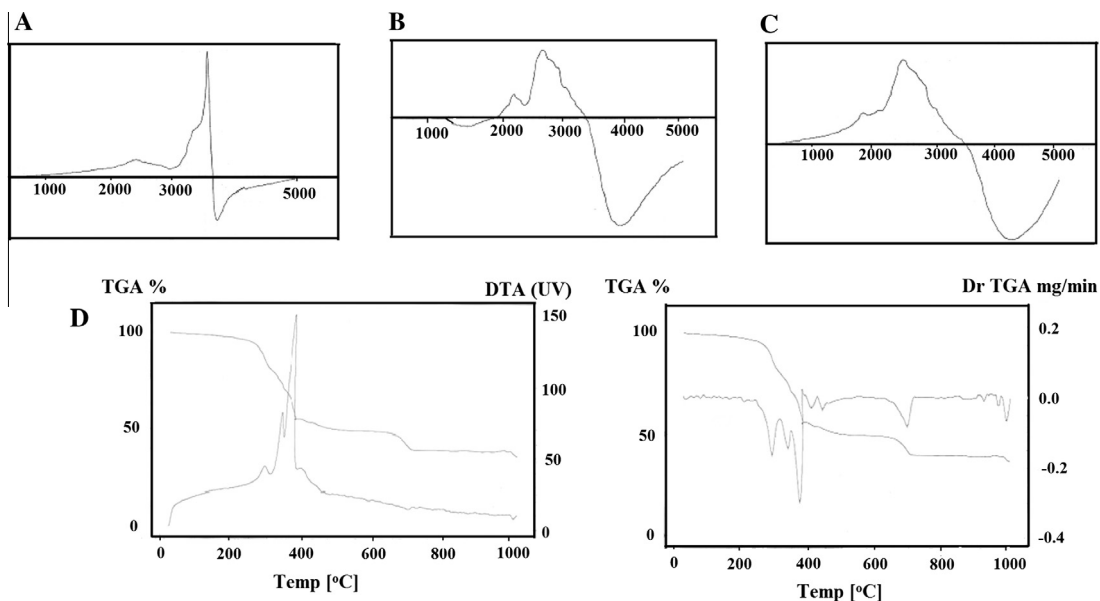


Fig. 2. (A) ESR of Cu-HL1, (B) ESR of Cu-HL2, (C) ESR of Cu-HL3 and (D) DTG of Cu-HL3.

**Table 2**  
ESR spectral parameters of the synthesized Cu (II) complexes.

Compound	$g_{11}$	$g_{\perp}$	$G$	$\alpha^2$	$\Delta E$	
					$\Delta_{\parallel}$	$\Delta_{\perp}$
Cu-HL1	2.23	2.06	3.80	0.83	28,869	27,666
Cu-HL2	2.20	2.06	3.30	0.89	33,200	27,666
Cu-HL3	2.45	2.13	3.46	0.89	14,755	12,769

d- spacing values (1.26 to 2.54 Å) as shown in Fig. 3. This indicates the crystalline nature of the synthesized oxides.

#### FT-IR of CuO

The FT-IR spectra (Fig. 4) showed several significant absorption peaks. The broad absorption bands in the range of 519–592  $\text{cm}^{-1}$  is assigned to Cu–O stretching vibration mode while, the broad

absorption band centered at 3440  $\text{cm}^{-1}$  is attributable to the band O–H stretching vibrations and the weak band near 1634  $\text{cm}^{-1}$  is assigned to H–O–H bending vibrations mode were also presented due to the adsorption of water in air when FT-IR sample disks were prepared in an open air [75].

#### Optical properties of CuO

UV-Vis absorption spectra were carried out in order to characterize the optical absorbance properties of the prepared CuO nanoparticles, as presented in Fig. 4. The band gap ( $E_g$ ) can be calculated using the following equation:

$$(\alpha h\nu)^n = K(h\nu - E_g)$$

where  $\alpha$  is the absorption coefficient,  $K$  is a constant,  $E_g$  is the band gap and  $n$  equals either 1/2 for an indirect allowed transition or 2 for a direct allowed transition. For the prepared CuO nanoparticles,  $(\alpha h\nu)^2$  is plotted versus  $h\nu$ , as shown in Fig. 4. The extrapolation of

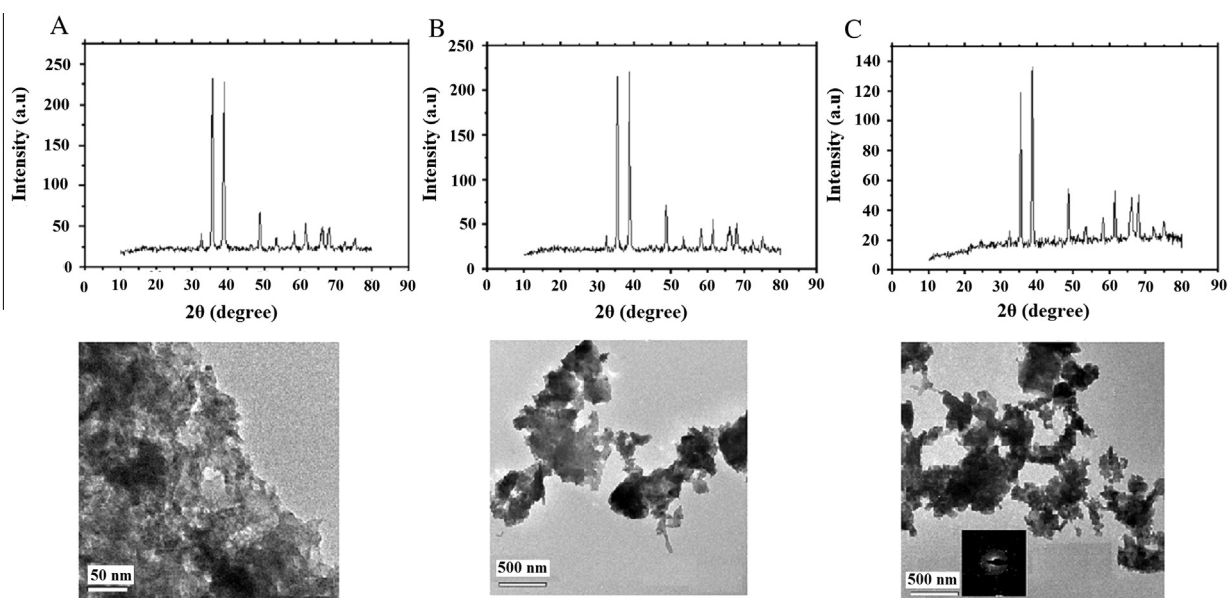
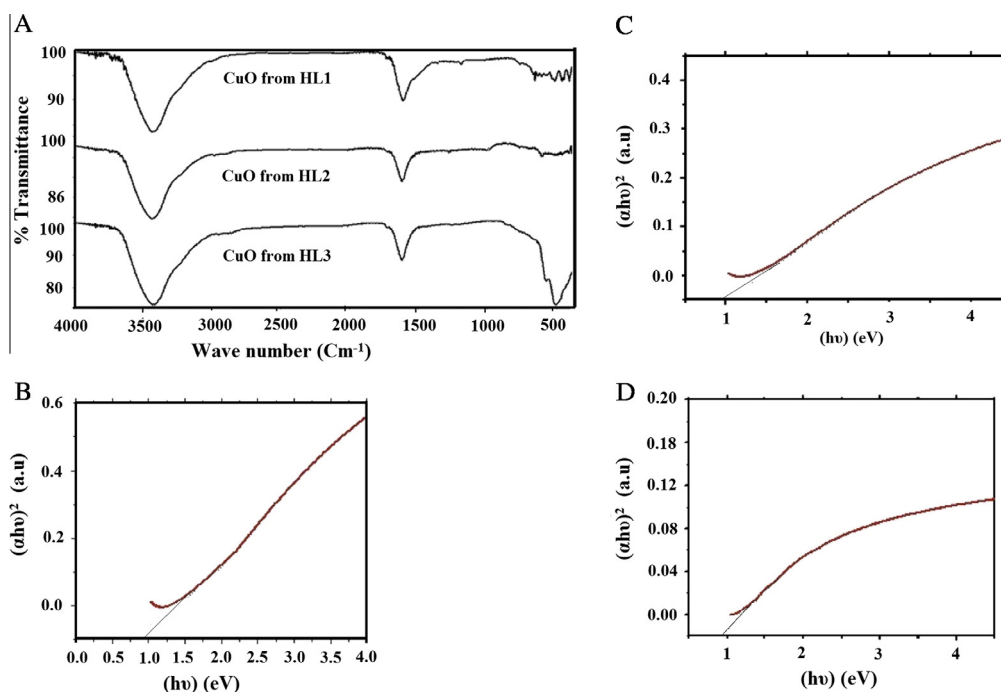


Fig. 3. XRD and HR-TEM of CuO prepared using Cu (II) complex of (A) HL1, (B) HL2 and (C) HL3.



**Fig. 4.** (A) FT-IR of CuO prepared using **HL1**, **HL2** and **HL3**, (B) optical energy gap of CuO prepared using **HL1**, (C) optical energy gap of CuO prepared using **HL2** and (D) optical energy gap of CuO prepared using **HL3**.

each graph to  $(\alpha h\nu)^2 = 0$  yields the optical direct band gaps ( $E_g$ ) which were found 0.96, 1.00 and 0.98 eV for CuO nanoparticles prepared using Cu (II) complexes of **HL1**, **HL2** and **HL3**, respectively. These values reveal that the as-prepared CuO nanoparticles products are semiconductors and are in a good agreement with the reported data [76].

### Biological activities

All the synthesized Schiff bases (**HL1**, **HL2** and **HL3**), their Cu (II) complexes and as-prepared CuO nanoparticles were screened in vitro for their biological activities using bacteria (*E. coli* & *S. aureus*) and fungi (*A. flavus* & *C. albicans*). Ampicillin (antibacterial agent) and Amphotericin B (antifungal agent) served as positive controls for antimicrobial activity and filter disc impregnated with 10  $\mu$ L of solvent (DMSO) was used as negative control. During incubation time, the tested chemical diffuses from the disc into the agar; only around the disc. When the organism is susceptible to the chemical, it will not grow in an area around the disc. This area of no growth, known as “**zone of inhibition**”, was measured and tabulated in Table 3. All tested compounds showed moderate activity against both pathogenic bacteria strains and poor antifungal activity. All Cu (II) complexes and CuO nanoparticles showed no activity on both of *A. flavus* and *C. albicans* fungi.

### Photocatalytic activity of CuO nanoparticles

The methylene blue dye degradation over the as-prepared CuO, prepared using Cu (II)-**HL3**, under UV illumination in the presence of  $H_2O_2$  was studied to investigate the photocatalytic activity via photo Fenton reaction [49–55]. However, it is worthy to mention that CuO product prepared using Cu (II)-**HL3** has specifically been chosen, in order to exploit high surface area of this product because it has the lowest crystallite size (28.28 nm). The UV-Vis spectra of the decomposed MB dye at different reaction times (from 0 to 8 h) under UV illumination in the presence of  $H_2O_2$  were

**Table 3**

The antimicrobial activity (in vitro) of synthesized Schiff bases, their Cu (II) complexes and their copper oxides.

Compound	Bacteria		Fungi	
	<i>E. coli</i> ( $G^-$ )	<i>S. aureus</i> ( $G^+$ )	<i>A. flavus</i>	<i>C. albicans</i>
<b>HL1</b>	9	10	0.0	0.0
<b>HL2</b>	12	10	9	10
<b>HL3</b>	11	11	9	9
Cu- <b>HL1</b>	0.0	0.0	0.0	0.0
Cu- <b>HL2</b>	0.0	9	0.0	0.0
Cu- <b>HL3</b>	0.0	0.0	0.0	0.0
CuO from <b>HL1</b>	10	11	0.0	0.0
CuO from <b>HL2</b>	10	11	0.0	0.0
CuO from <b>HL3</b>	10	11	0.0	0.0

depicted in Fig. 5(A and B). Fig. 5(A and B) shows that the dye exhibits an absorption peak at 664 nm and the absorption intensity of the dye solution gradually decreases with the increase of exposed time, indicating a decrease in the MB dye concentration which consequently means the effective photodegradation of the dye using CuO catalyst under UV illumination in the presence of  $H_2O_2$ . This study revealed that almost 96.18% of the MB dye decomposed under UV illumination in the presence of  $H_2O_2$  within 6 h which is considered a very high percent compared with others in literature [49–64]. Several experiments were carried out to degrade MB dye solution in the presence or absence of UV light and with or without oxidant or catalyst but the results showed that the photolysis of the dye was negligible (~5–10%) (Figures omitted for brevity). Photodegradation reaction mechanism in the presence of UV only, (Catalyst + UV) and (UV + Catalyst +  $H_2O_2$ ) has been clarified in Scheme 2. After absorbing UV-light only, the excited MB reduces  $O_2$  to  $O_2^-$ , which in turn reacts with a proton (from the autoprotolysis of the solvent water) to produce  $OOH$ . In total, the cationic dye radical is degraded to carbon dioxide, water and mineral acids via intermediate. They also explained  $OOH$  and  $OH$ , which are necessary for the complete degradation of the dye

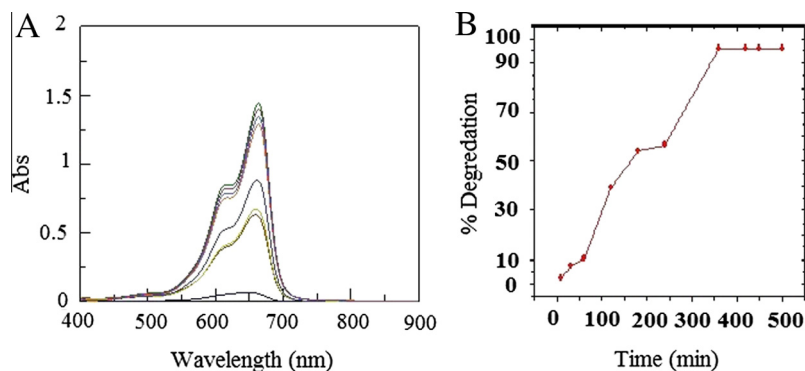
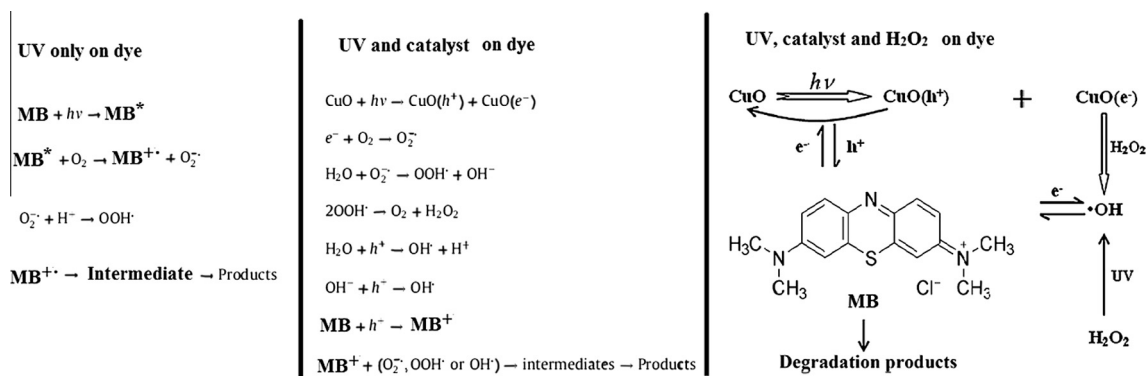


Fig. 5. (A) Photocatalytic degradation of MB dye using CuO prepared using HL3 and (B) % degradation versus time.



Scheme 2. Proposed reactions for the photodegradation of MB dye in the presence of UV only, (Catalyst + UV) and (UV + Catalyst + H<sub>2</sub>O<sub>2</sub>).

[49,52]. Photocatalytic degradation of MB dye in the presence of (Catalyst + UV) usually includes the separation of electron hole pairs and the subsequent reduction–oxidation reactions under UV-light irradiation, electrons and holes are generated on the surface of CuO. The electrons scavenged by the adsorbed molecular oxygen species, and the holes trapped by water or adsorbed MB molecules. Then MB dye is degraded directly by photogenerated oxidants [49,52] such as  $O_2^{\bullet-}$ ,  $\bullet OOH^{\bullet}$  and  $\bullet OH$ . Adding  $H_2O_2$  in the presence of catalyst and UV increases the photodegradation rate of MB dye because the direct decomposition of  $H_2O_2$  under UV light produces  $\bullet OH$ , which directly oxidize MB dye as shown in Scheme 2. It is noteworthy that the advantage of using nanosized CuO in the degradation of MB dye over other copper salts is that they are insoluble in water, nonpoisonous, highly surface area and reusability performance [49–55].

## Conclusion

The Cu (II) complexes were synthesized by the reaction of the newly prepared 3-R-1,2,4-triazole Schiff bases (R = H, CH<sub>3</sub> or C<sub>2</sub>H<sub>5</sub>) with CuCl<sub>2</sub>·2H<sub>2</sub>O in 1:1 M ratio in the presence of sodium acetate trihydrate at reflux temperature. The synthesized Cu (II) complexes were characterized using elemental analysis, molar conductivity, FT-IR, magnetic moment, ESR, DTG analysis, and UV–Vis spectroscopy. CuO nanoparticles were synthesized via thermal decomposition of newly prepared Cu (II) triazole Schiff base complexes, as solid precursors. The as-prepared CuO nanoparticles were characterized using XRD, HR-TEM, FT-IR and optical properties. By this fast and simple method, CuO nanoparticles can be produced without expensive and toxic solvents or complicated equipment. The crystal size was found 35.60, 34.47 and

28.28 nm whereas, the optical energy gap was found 0.96, 1.00 and 0.98 eV for CuO nanoparticles prepared using Cu (II) complexes of HL1, HL2 and HL3, respectively. The as-prepared CuO using HL3 (Lowest particle size = 28.28 nm) was studied for the photocatalytic degradation of methylene blue dye (MB) under UV illumination in the presence of H<sub>2</sub>O<sub>2</sub> and the results revealed that almost 96.18% of the MB dye was decomposed within 6 h. All Schiff bases, their Cu (II) complexes and CuO nanoparticles showed moderate activity against both pathogenic bacteria strains (*E. coli* & *S. aureus*) and poor antifungal activity (*A. flavus* & *C. albicans*).

## References

- [1] S. Spyroula, P. Garoufalla, E. Tani, O. Todoulou, A. Papadaki-Valiraki, E. Filippatos, E. Clercq, P.N. Kourounakis, *J. Pharm. Pharmacol.* 50 (1998) 117–124.
- [2] S.N. Sambrekar, S.A. Patil, *Int. J. Pharm. Biomed. Sci.* 2 (2) (2011) 520–524.
- [3] K. Zamani, K. Faghihi, M.R. Sangi, J. Zolgharnein, *Turk. J. Chem.* 27 (2003) 119–125.
- [4] S. Desai, U. Laddi, R. Bennur, B. Bennur, *Indian J. Chem.* 52B (2013) 1176–1181.
- [5] V.N. Bercean, I.V. Ledeti, V. Badea, M. Balan, C. Csunderlik, *Rev. Chim. (Bucharest)*, 61 (2010) 1028–1030.
- [6] S.R. Desai, U. Laddi, R.S. Bennur, P.A. Patil, S. Bennur, *Indian J. Pharm. Sci.* 73 (1) (2011) 115–120.
- [7] M.A. Quraishi, *Corros. Sci.* 70 (2013) 161–169.
- [8] C. Zeng, F. Liu, D. Ping, Y. Cai, R. Zhong, J.Y. Becker, *J. Electroanal. Chem.* 625 (2009) 131–137.
- [9] P.D.R. Kumari, J. Nayak, A.N. Shetty, *Synth. React. Inorg. Met. Org. Chem.* 41 (2011) 774–784.
- [10] B.S. Holla, B. Veerendra, M.K. Shivananda, B. Poojary, *Eur. J. Med. Chem.* 38 (2003) 759–767.
- [11] H. Bayrak, A. Demirbas, H. Bektas, S. Karaoglu, N. Demtrbas, *Turk. J. Chem.* 34 (2010) 835–846.
- [12] Chandramouli, M.R. Shivanand, T.B. Nayanbhai, Bheemachari, R.H. Udipi, *J. Chem. Pharm. Res.* 4 (2) (2012) 1151–1159.
- [13] A.K. Wahi, A.K. Singh, A. Singh, *Der. Pharm. Chem.* 3 (5) (2011) 46–154.

- [14] S.U. Cicekli, T. Onkol, S. Ozgen, M.F. Sahin, *Rev. Roum. Chim.* 57 (3) (2012) 187–195.
- [15] H. Khanmohammadi, M. Erfantalab, G. Azimi, *Spectrochim. Acta. A* 105 (2013) 338–343.
- [16] R. Zhang, Q. Wang, Q. Li, C. Maa, *Inorg. Chim. Acta.* 362 (2009) 2762–2769.
- [17] A.K. Singh, O.P. Pandey, S.K. Sengupta, *Spectrochim. Acta. A* 85 (2012) 1–6.
- [18] K. Singh, M.S. Barwa, P. Tyagi, *Eur. J. Med. Chem.* 41 (2006) 147–153.
- [19] G.B. Bagihalli, P.G. Avaji, S.A. Patil, P.S. Badami, *Eur. J. Med. Chem.* 43 (2008) 2639–2649.
- [20] K. Singh, Y. Kumar, P. Puri, M. Kumar, C. Sharma, *Eur. J. Med. Chem.* 52 (2012) 313–321.
- [21] M. Ghassemzadeh, L. Fallahnejad, M.M. Heravi, B. Neumüller, *Polyhedron* 27 (2008) 1655–1664.
- [22] M.L. Sharma, S.K. Sengupta, O.P. Pandey, *Spectrochim. Acta. A* 95 (2012) 562–568.
- [23] G.J. Kharadi, *Spectrochim. Acta. A* 110 (2013) 311–316.
- [24] K. Singh, Y. Kumar, C. Sharma, *Acta. A. Mol. Biomol. Spectrosc.* 75 (2010) 98–105.
- [25] N.S.A.M. Khalil, *Eur. J. Med. Chem.* 45 (2010) 5265–5277.
- [26] I.R. Mostafa, G.M. Al-Wakiel, N.A. Fathalla, S. Kamal, *Chin. J. Chem.* 30 (2012) 547–556.
- [27] K. Singh, P. Puri, Y. Kumar, C. Sharma, K.R. Aneja, *Bioinorg. Chem. Appl.* 654250 (2011) 1–10.
- [28] K. Singh, Y. Kumar, P. Puri, G. Singh, *Bioinorg. Chem. Appl.* 729708 (2012) 1–9.
- [29] A. Sharma, T. Mehta, Manish K. Shah, *Der. Chem. Sinica* 4 (1) (2013) 41–146.
- [30] M.M.H. Khalil, E.H. Ismail, G.G. Mohamed, E.M. Zayed, A. Badr, *Open. J. Inorg. Chem.* 2 (2012) 13–21.
- [31] G.G. Mohamed, M.M. Omar, A.M. Hindy, *Turk. J. Chem.* 30 (2006) 361–382.
- [32] M.V. Angelusiu, G.L. Almăjan, D.C. Ilies, T. Rosu, M. Negoiu, *Chem. Bull. "Politehnica" Univ. (Timisoara)* 53 (2008) 78–82.
- [33] S. Chandra, R. Kumar, *Spectrochim. Acta. A* 61 (2005) 437–446.
- [34] K. Thangavelu, K. Parameswari, K. Kuppusamy, Y. Haldorai, *Mater. Lett.* 65 (2011) 1482–1484.
- [35] S. Farhadi, K. Pourzare, S. Sadeghinejad, *J. Nanostruct. Chem.* 3 (16) (2013) 1–7.
- [36] S. Farhadi, J. Safabakhsh, *J. Alloys Compd.* 515 (2012) 180–185.
- [37] F. Mohandes, F. Davar, M. Alavati-Niasari, *J. Magn. Magn. Mater.* 322 (2010) 872–877.
- [38] M. Salavati-Niasari, Z. Fereshteh, F. Davar, *Polyhedron* 28 (2009) 1065–1068.
- [39] A. Hosseini, S. Jabbari, H.R. Rahimpour, A.R. Mahjoub, *J. Mol. Struct.* 1028 (2012) 215–221.
- [40] M.Y. Nassar, A.S. Attia, K.A. Alfalou, M.F. El-Shahat, *Inorg. Chim. Acta.* 405 (2013) 362–367.
- [41] S. Farhadi, K. Pourzare, *Mater. Res. Bull.* 47 (2012) 1550–1556.
- [42] M.Y. Nassar, T.Y. Mohamed, I.S. Ahmed, *J. Mol. Struct.* 1050 (2013) 81–87.
- [43] O.B. Ibrahim, M.A. Mohamed, M.S. Refat, *Can. Chem. Trans.* 2 (2014) 108–121.
- [44] F. Behnoudnia, H. Dehghani, *Polyhedron* 56 (2013) 102–108.
- [45] H. Thakuria, G. Das, *Polyhedron* 26 (2007) 149–153.
- [46] Y. Haldorai, J. JinShim, *Mater. Lett.* 116 (2014) 5–8.
- [47] Z. Yang, D. Wang, F. Li, D. Liu, P. Wang, X. Li, H. Yue, S. Peng, D. He, *Mater. Lett.* 90 (2013) 4–7.
- [48] A. Pendashteh, M.S. Rahmanifar, M.F. Mousavi, *Ultrason. Sonochem.* 21 (2014) 643–652.
- [49] J. Li, F. Sun, K. Gu, T. Wu, W. Zhai, W. Li, S. Huang, *Appl. Catal. A: Gen.* 406 (2011) 51–58.
- [50] H. Shi, Y. Zhao, Na. Li, K. Wang, X. Hua, M. Chen, F. Teng, *Catal. Commun.* 47 (2014) 7–12.
- [51] S.P. Meshram, P.V. Adhyapak, U.P. Mulik, D.P. Amalnerkar, *Chem. Eng. J.* 204–206 (2012) 158–168.
- [52] B. Shaabani, E. Alizadeh-Gheshlaghi, Y. Azizian-Kalandaragh, A. Khodayari, *Adv. Powder. Technol.* 25 (2014) 1043–1052.
- [53] M.U.A. Prathap, B. Kaur, R. Srivastava, *J. Colloid. Interf. Sci.* 370 (2012) 144–154.
- [54] Q. Shao, L. Wang, X. Wang, M. Yang, S. Ge, X. Yang, J. Wang, *Solid. State. Sci.* 20 (2013) 29–35.
- [55] M. Zhu, D. Meng, C. Wang, J. Di, G. Diao, *Chin. J. Catal.* 34 (2013) 2125–2129.
- [56] M.H. Habibi, B. Karimi, *J. Ind. Eng. Chem.* 20 (2014) 925–929.
- [57] C. Li, Y. Yin, H. Hou, N. Fan, F. Yuan, Y. Shi, Q. Meng, *Solid. State. Commun.* 150 (2010) 585–589.
- [58] R. Wu, Z. Ma, Z. Gu, Y. Yang, *J. Alloys Compd.* 504 (2010) 45–49.
- [59] C. Ma, L. Zhu, S. Chen, Y. Zhao, *Mater. Lett.* 108 (2013) 114–117.
- [60] K.S. Siddiqi, S. Khan, S.A.A. Nami, M.M. El-ajaily, *Spectrochim. Acta. A* 67 (2007) 995–1002.
- [61] F. Audrieth, E.S. Scott, P.S. Kippur, *J. Org. Chem.* 19 (1954) 733–736.
- [62] R. Smicius, M.M. Burbuliene, V. Jakubkiene, E. Udrenaitė, P. Vainilavicius, *J. Heterocycl. Chem.* 44 (2007) 279–284.
- [63] H. Yu, J. Ma, G. Xu, S. Li, J. Yang, Y. Liu, Y. Cheng, *J. Organomet. Chem.* 691 (2006) 3531–3539.
- [64] A.W. Bauer, W.M. Kirby, C. Sherris, M. Turck, *Am. J. Clin. Pathol.* 45 (1966) 493–496.
- [65] M.A. Pfaller, L. Burmeister, M.A. Bartlett, M.G. Rinnaldi, *J. Clin. Microbiol.* 26 (1988) 1437–1441.
- [66] R.M. Silverstein, F.X. Webster, D.J. Kiemle, *Spectroscopic Identification of Organic Compounds*, 7th edn., John Wiley & Sons Inc., USA, 2005.
- [67] F.A. Miller, D.W. Mayo, R.W. Hannah, *Course Notes on the Interpretation of Infrared and Raman Spectra*, John Wiley & Sons Inc., USA, 2003.
- [68] B.K. Sinha, M. Kumar, R. Kumar, N.C. Bhattacharjee, *J. Indian Chem. Soc.* 72 (1995) 623–625.
- [69] H. Khanmohammadi, M.H. Abnosi, A. Hosseinzadeh, M. Erfantalab, *Spectrochim. Acta. A* 71 (2008) 1474–1477.
- [70] B. Gangadhar, Bagihalli, S.A. Patil, *J. Coord. Chem.* 62 (2009) 1690–1700.
- [71] S.L. Reddy, T. Endo, G.S. Reddy, *Advanced Aspects of Spectroscopy*, Chapter 1, 2012, pp. 1–15.
- [72] Z.S. Chickneyan, A.L. Briseno, X. Shi, S. Han, J. Huang, F. Zhou, *J. Nanosci. Nanotech.* 4 (2003) 1–5.
- [73] Z.S. Chickneyan, A.L. Briseno, X. Shi, S. Han, J. Huang, F. Zhou, *J. Nanosci. Nanotech.* 4 (2003) 1–7.
- [74] J. Feng, H.C. Zeng, *Chem. Mater.* 15 (2003) 2829–2831.
- [75] K. Kannaki, P.S. Ramesh, D. Geetha, *Int. J. Sci. & Eng. Res.* 3 (9) (2012) 1–7.
- [76] G. Grivani, S. Delkhosh, K. Fejfarová, M. Dušek, A.D. Khalaji, *Inorg. Chem. Commun.* 27 (2013) 82–85.